Excess of low-frequency modes in Lennard-Jones systems

2002 J. Phys.: Condens. Matter 14 L393

(http://iopscience.iop.org/0953-8984/14/22/102)

INSTITUTE OF PHYSICS PUBLISHING JOURNAL OF PHYSICS: CONDENSED MATTER

J. Phys.: Condens. Matter **14** (2002) L393–L398 PII: S0953-8984(02)34058-X

LETTER TO THE EDITOR

Excess of low-frequency modes in Lennard-Jones systems

Alberto De Santis[1], **Alessandro Ercoli**[1] **and Dario Rocca**[2]

[1] Facoltà di Agraria, DISA and INFM-Viterbo, Università della Tuscia, Via San Camillo De Lellis, 01100 Viterbo, Italy
[2] Dipartimento di Fisica and INFM-Roma I, Università di Roma I 'La Sapienza', Piazzale Aldo Moro 2, 00185 Roma, Italy

Received 20 February 2002, in final form 2 May 2002
Published 23 May 2002
Online at stacks.iop.org/JPhysCM/14/L393

Abstract

Argon dynamics is simulated in the glassy state at the temperature of 20 K. A fast quenching is used to study the slow time evolution from the glass to the crystalline state. Observation of the crystallization process reveals the growth of temperature, a rapid change in the mean square displacement, and strong variations in the relative pair dynamics. Our main results are: (a) detecting the presence of a low-frequency mode in the pair dynamics of the glass; (b) showing that this mode is responsible for the intensity excess at low frequency in the power spectrum (compared to that of the crystal); and (c) showing that it decreases more and more as the crystallization proceeds.

The properties of glasses and supercooled liquids have been widely investigated in recent years [1–4]. The glass shows typical behaviours that are absent in the crystal, such as the spectral intensity excess at low energies (the boson peak) detected by some scattering experiments. The related translational density of states (DOS) shows state excess with respect to the Debye model predictions. Many mechanisms have been proposed to explain the boson peak formation [1,4–10] (propagating, localized, extended non-propagative modes, etc) depending on the glass temperature, materials, and quenching history. In monatomic systems, several simulation studies have been devoted to the glass formation. For soft spheres [11] and Lennard-Jones (LJ) [12] fluids, the critical quenching rate is about 10^{12} K s^{-1}. For greater values, soft-sphere glasses exhibit a crystallization tendency that becomes stronger as the quenching rate becomes faster [11], while binary LJ mixtures show a weak dependence on fast cooling rates [13]. For one-component LJ (1LJ) systems, it is very easy to obtain crystallization [14], and attempts to study the long-time dynamics of the glass can be frustrated by the unwanted formation of small crystals. Consequently, the dynamics and structure of 1LJ disordered systems have been investigated only for a few tenths of a picosecond [15], or at very low temperatures [16], or by adding a many-body term to the potential in order to stabilize the amorphous state [17]. Other problems derive from the molecular

dynamics simulation technique. The periodic boundary conditions can induce 'catastrophic' crystallization processes [18] and the finite size of the simulated samples produces spurious effects which are mainly relevant in strong glass formers [7, 19].

In this work, we exploit the propensity of the 1LJ system to show crystallization, with the aim of studying the evolution of structural and dynamical properties as the crystallization proceeds. To obtain a glassy argon ($T = 20$ K) which should slowly evolve towards the crystal, we used a fast quenching rate, as in the case of soft spheres [11]. We show that a low-frequency mode yields an excess in the DOS, and could be related to the boson peak formation[3]. The evidence of a DOS excess is obtained by comparing the behaviour of disordered, crystalline and Debye-like systems, while the boson peak connection is suggested by the time decrease of the low-frequency mode intensity and by its disappearance when the crystallization process is over. These results are obtained by applying a methodology proposed for supercooled water states [20] and recently extended to normal liquid states [21].

Molecular dynamics simulations at constant density were carried out for 864 atoms interacting via LJ potential ($\epsilon/K = 119.8$ K, $\sigma = 3.405$ Å) in a cubic box with periodic boundary conditions. Firstly, the configurations of the liquid near the triple point ($T = 85$ K, $\rho = 1.42$ g cm^{-3}) (melting state, for simplicity) were produced; then, the supercooled ($T = 55$ K) and quenched ($T = 20$ K) states were simulated at the triple-point density of the liquid. The perfect-crystal solid state at 20 K was reached by starting from the 0 K fcc lattice. For all the runs, after equilibration, the configurations were stored every four time steps, the time step being of 5 fs. The quenched state history is: ultrafast cooling of the triple-point liquid to 20 K (first time step) and temperature scaling at every step for 1000 steps (average quenching rate an order of magnitude faster than the critical rate); 90 000 steps with temperature scaling at every 5000 steps; free evolution of the system and configuration recording in time windows of 10 000 steps (50 ps) until crystallization is achieved. The further evolution up to 1 ns was followed, and the two final 50 ps time window configurations were recorded. Since the quenching rate used was faster than the critical one and the temperature of 20 K was lower than the glass transition temperature [17], we expected to produce states stable enough to make equilibrium averages significant (quasi-stable states). The same quenching procedure was applied to a sample of 4000 atoms and similar processes were observed. Checks with 4000-atom samples were also made for all the other equilibrium states. A sample vitrified with a quenching rate close to the critical one ($\sim 10^{12}$ K s^{-1}) was also produced. In the first time window of 50 ps, practically the same structural and dynamics properties were observed.

In the framework of a vibrational mode approach, the interparticle separation vector can be written as $\boldsymbol{R}_{ij}(t) = \boldsymbol{R}_{ij}(0) + \boldsymbol{A}_{ij,n}\chi_n(t)$, $\boldsymbol{A}_{ij,n}$ being the amplitude vector and χ_n the nth normal mode; summing over repeated indexes is implied. To study the dynamics along R_{ij} (the longitudinal component), one defines the correlation function $B(r_0; t) = \langle \boldsymbol{R}_{ij}(t) \cdot \boldsymbol{u}_{ij}(0) - R_{ij}(0)\rangle_0 / \langle R_{ij}(0)\rangle_0$, where $\boldsymbol{u}_{ij}$ is the unit vector in the $\boldsymbol{R}_{ij}$-direction and $\langle\ \rangle_0$ stands for the average over tagged pairs which, at the initial time, have the separation $r_0 = R_{ij}(0)$ inside the range r_1–r_2. The kinematic equation for χ_n is $A^p_{ij,n}\chi_n(t) = Q_n \cos(\omega_n t) + V_n \sin(\omega_n t)/\omega_n$, where $A^p_{ij,n} = \boldsymbol{A}_{ij,n} \cdot \boldsymbol{u}_{ij}(0)$, $Q_n = A^p_{ij,n}\chi_n(0)$, $V_n = A^p_{ij,n}\dot{\chi}_n(0)$, and where ω_n and $\dot{\chi}_n(0)$ are the frequency and the initial velocity of the nth mode, respectively. The average of V_n vanishes for the equilibrium distribution of the initial velocities. To derive vibrational modes, one introduces selection in the pair velocities and distinguishes between approaching (in) and departing (out) pairs. The averages of Q_n and $Q_n^{(\mathrm{out})}$ coincide because they depend on the coordinate distribution only. By subtracting $B^{(\mathrm{out})}(r_0; t)$ from $B(r_0; t)$ [20], one obtains

[3] We have found that the low-frequency mode is present also in supercooled liquid argon ($T = 55$ K) and in the liquid near to the melting point ($T = 85$ K).

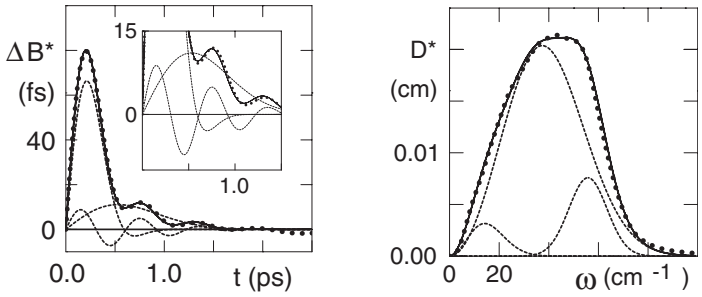

Figure 1. $\Delta B^*(r_0; t)$ and the corresponding DOS, $D^*(\omega)$, for $0 < r_0 < 5.1$ Å. Below the total curve from molecular dynamics (solid curve), vibrational components are shown. Their sum is the best fit to the total molecular dynamics curve, indicated by the dots superimposed on the solid curve. The inset shows details of the curves.

the function $\Delta B(r_0; t) = \langle V_n^{(\mathrm{out})} \sin(\omega_n t)/\omega_n \rangle_0$, which contains the mode dynamics. The related DOS is[4] $D(\omega) = \int \Delta B(r_0; t)\, \omega \sin(\omega t)\, \mathrm{d}t$. Figure 1 shows $\Delta B^*(r_0; t)$ obtained from molecular dynamics (the star stands for normalization to the DOS area) for Ar after the quenching at 20 K. In this work, only the pairs initially lying in the first coordination shell are considered ($0 < r_0 < 5.1$ Å). In the liquid state, the long-time $\Delta B^*(r_0; t)$ yields a plateau whose height, $A^*(r_0)$, decreases with the temperature. The plateau is related to non-vibrational contributions, and its height is proportional to the relative pair diffusion coefficient[5]. The phenomenological expression used to represent the total $\Delta B^*(r_0; t)$ is [21]

$$\Delta B^*(r_0; t) = \sum_m x_m^* \sin(\omega_m t) \exp[-(t/\tau_m)^2] + A^*(r_0)[1 - \exp(-t/\tau_e)]. \quad (1)$$

The index m runs over damped harmonic oscillator (DHO)-like functions [23] modelling vibrational contributions, while the second term represents relaxations towards diffusion. In a quenched state the diffusion is negligible, and $A^*(r_0)$ vanishes. Equation (1), with $A^*(r_0) = 0$, was best fitted to the $\Delta B^*(r_0; t)$ produced by molecular dynamics. The m-index runs over three DHO functions. In the fit procedure, two DHO functions were constrained to produce peaks around the main solid frequencies at 60 cm^{-1} (Debye frequency) and 40 cm^{-1} (Einstein frequency). The best fitted components of equation (1) and the corresponding DOS are shown in figure 1. As is seen, the fit quality is good; the need for three independent DHO functions is quite evident from the $\Delta B^*(r_0; t)$ shape. A DHO mode is necessary to account for the first peak around 0.2 ps; in the frequency domain, it yields the band centred around the Einstein frequency. This is the main DOS component present in the states investigated (the perfect-crystal solid included; see figure 2). A second mode is *necessary* to produce the tail between 0.5 and 1.5 ps; it yields the DOS band below 20 cm^{-1}. Note that in the frequency domain, this mode appears as a detail and is hardly detectable. The third mode is the fastest oscillation giving rise to the band at about 60 cm^{-1}; it is clearly visible in $\Delta B^*(r_0; t)$ as a fast modulation of the tail between 0.5 and 1.5 ps (see the inset of figure 1), and in the crystallized state (see later, figure 2).

The time evolution of the 20 K quenched argon was monitored by computing $\Delta B^*(r_0; t)$ (figure 2), the radial pair distribution function $g(r)$, and the mean square displacements (figure 3) over 50 ps time windows. For every window, one resets the time, as is usual in studying non-ergodicity and long-time ageing effects [1,24,25], and computes averages over a

[4] The term DOS is used to indicate the power spectrum of $\omega \Delta B(r_0; t)$ that yields part of the total DOS defined as the cosine Fourier transform of the velocity autocorrelation function [21].

[5] It can be shown that this is true in the cases of water [21] and argon [22] liquid.

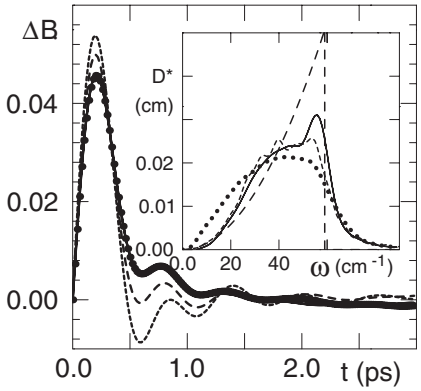

Figure 2. The results of monitoring, in time windows of 50 ps, the time evolution of the 20 K quenched state of argon via the dynamical behaviour of $\Delta B(r_0; t)$, for $0 < r_0 < 5.1$ Å. Dots: 1° window (0–50 ps); solid curve: average of ΔB over the first eight time windows; long-dashed curve: 11° window; short-dashed curve: 12° window. The inset shows the DOS of: glassy argon (DOS-1 (dots)), crystallized solid (DOS-12 (short-dashed curve)), perfect-crystal solid (DOS-fcc (solid curve)), Debye model predictions (long-dashed curve).

limited time interval (usually, the first 20 ps) as for the equilibrium states (quasi-equilibrium). This is correct if one studies just the fast dynamics [26]. In figure 2, one can see that $\Delta B^*(r_0; t)$ is practically unchanged over many time windows. In the 11° one (500 ps), $\Delta B^*(r_0; t)$ shape changes rapidly, since the contribution of the low-frequency mode decreases. In the 12° one, the low-frequency mode vanishes and $\Delta B^*(r_0; t)$ is stable up to 1 ns. The behaviour of $g(r)$ and the mean square displacements are shown in figure 3. In the 1° time window, broad secondary $g(r)$ peaks and a vanishing diffusivity can be observed. At 550 ps, the linear mean square displacement time dependence (diffusivity) and the formation of $g(r)$ sharp peaks around 5.3 Å [27] indicate a crystallization process. This is also supported by the catastrophic temperature behaviour shown in figure 3. This behaviour follows previous findings [18], and similar effects have been found in soft-sphere glasses [28] too. Our results show that the decrease of low-frequency mode (figure 2) and the diffusion growth (figure 3) accompany the increase of temperature. This should suggest that the low-frequency mode relaxes and releases heat, leading to rising temperature and mobility, and produces crystallization. But, if one averages over smaller time windows around the 'catastrophe' at 550 ps, one finds that the system has practically crystallized, whereas the diffusivity is still a maximum (see also the 12° time window data of figure 3). An explanation of this requires further analyses, probably addressed to the study of chainlike [28] or stringlike motions and mobile and immobile particle clusters [29].

To gain more insight, it is worth studying $\Delta B^*(r_0; t)$ for the fcc perfect crystal at 20 K. In the inset of figure 2, the DOS produced by the quenched argon in the 1° (DOS-1) and 12° (DOS-12) windows and the perfect-crystal fcc DOS (DOS-fcc) are compared. Figure 2 also shows the quadratic dependence of the Debye DOS. As is seen from figure 2, DOS-fcc and DOS-12 are quite similar. The first one has a sharper peak around 59 cm^{-1}, the Debye frequency. With respect to DOS-1, both show a lack of intensity around 10 cm^{-1} and an excess around 59 cm^{-1}. Usually, one plots $f^*(\omega) = D^*(\omega)/\omega^2$ to show the excess of the DOS intensity with respect to the constant value predicted by the Debye model and to detect the formation of a peak. As is seen in figure 4, the low-frequency excess of $f^*(\omega)$ decreases

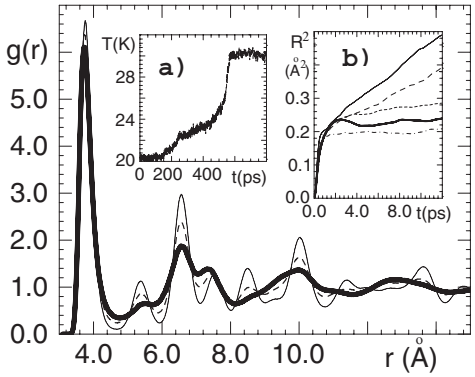

Figure 3. Pair distribution functions, $g(r)$, obtained from the 1° time window (0–50 ps) (bold solid curve) and from the average of the first eight time windows $g(r)$ (practically coincident with the bold solid curve); dashed and thin solid curves represent $g(r)$ for the 11° and 12° time windows, respectively. The $g(r)$ of the 20° window (not shown) coincides with the 12° one. Inset (a) shows the global temperature evolution and inset (b) the curves of the mean square self-displacement ($R^2(t) = \langle[\boldsymbol{R}_i(t) - \boldsymbol{R}_i(0)]^2\rangle$) for 1° (bold solid curve), 6° (short-dashed curve), 11° (dashed curve), 12° (thin solid curve), and 20° (dotted–dashed curve) time windows.

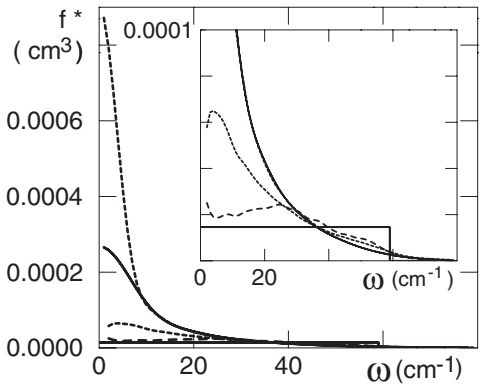

Figure 4. $f^*(\omega) = D^*(\omega)/\omega^2$ for Ar: from top to bottom the curves refer to liquid at $T = 85$ K, supercooled liquid at $T = 55$ K, glassy solid ($T = 20$ K), and crystallized solid. Also shown is the constant trend predicted by the Debye model. The inset shows details of $f^*(\omega)$ at low intensity.

as the system evolves from the liquid state to the solid one[6]. In the crystallized state no excess is present, and $f^*(\omega)$ shows a nearly flat low-frequency behaviour as predicted by the Debye model. In the glass state, the diffusion vanishes, and the low-frequency excess produces a peak, probably connected with the boson peak[7]. The boson peak intensity decreases in going from strong to fragile glass formers [30]. To our knowledge, this peak has not been observed for 1LJ systems, although a coherent potential approximation, which exploits the 1LJ potential, has

[6] The states mentioned in the caption of figure 4 are the liquid near to the melting point ($T = 85$ K, unpublished) and the supercooled liquid ($T = 55$ K) [22].

[7] The $\Delta B(r_0; t)$ correlation function is related to the translational pair dynamics projected along the $\boldsymbol{u}_{ij}(0)$ direction (longitudinal dynamics). By projecting $\boldsymbol{R}_{ij}(t)$ along a direction perpendicular to $\boldsymbol{u}_{ij}(0)$, one could define a $\Delta B_t(r_0; t)$ related to the transverse pair dynamics. Preliminary results show that the intensity excess of the low-frequency mode is also present in $\Delta B_t(r_0; t)$ for the liquid and glass states, and disappears as the crystallization proceeds. Checks for different r_0-values indicate that these results are valid in general.

been used to show the presence of the boson peak [31]. To summarize, we have found that in the argon glass a low-frequency mode produces a DOS excess probably connected with the boson peak formation. The intensity of the low-frequency mode decreases as instability increases and crystallization proceeds, thus supporting the connection between the low-frequency DOS excess and the topological disorder of glasses [32].

Thanks are due to Professor F Sciortino for helpful discussions and a critical reading of the manuscript.

References

[1] Kob W 1999 *J. Phys.: Condens. Matter* **11** R85
[2] Cummins H Z 1999 *J. Phys.: Condens. Matter* **11** A95
[3] Götze W and Mayr M R 2000 *Phys. Rev.* E **61** 587
[4] Angell C A *et al* 2000 *J. Appl. Phys.* **88** 3113
[5] Masciovecchio C *et al* 2000 *Phys. Rev. Lett.* **85** 1266
[6] Kantelhardt J W, Russ S and Bunde A 2001 *Phys. Rev.* B **63** 064302
[7] Horbach J, Kob W and Binder C 2001 *Eur. Phys. J.* B **19** 531
[8] Tse J S *et al* 2000 *Phys. Rev. Lett.* **85** 3185
[9] Parshin D A and Laermans C 2001 *Phys. Rev.* B **63** 132203
[10] Taraskin S N and Elliott S R 1999 *Phys. Rev.* B **59** 8572
Taraskin S N and Elliott S R 2000 *Phys. Rev.* B **61** 12 017
[11] Jund P, Caprion D and Jullien R 1997 *Phys. Rev. Lett.* **79** 91
[12] Nosé S and Yonezawa F 1986 *J. Chem. Phys.* **84** 1803
[13] Vollmayr K, Kob W and Binder K 1996 *J. Chem. Phys.* **105** 4714
[14] Shneidman V A and Uhlmann D R 1998 *J. Non-Cryst. Solids* **86** 224
[15] Luchnikov V A *et al* 1995 *Phys. Rev.* B **51** 15 569
[16] Ruocco G *et al* 2000 *Phys. Rev. Lett.* **84** 5788
[17] Di Leonardo R *et al* 2000 *Phys. Rev. Lett.* **84** 6054
[18] Honeycutt J D and Andersen H C 1984 *Chem. Phys. Lett.* **108** 535
[19] Horbach J *et al* 1996 *Phys. Rev.* E **54** R5897
[20] De Santis A, Ercoli A and Rocca D 1999 *Phys. Rev. Lett.* **82** 3452
[21] De Santis A, Ercoli A and Rocca D 2001 *J. Chem. Phys.* **115** 6632
[22] De Santis A, Ercoli A and Rocca D 2001 Harmonic and anharmonic contributions to the relative pair dynamics in simple liquids *Italian Phys. Soc. Conf. Proc.* **76** 77
[23] Monaco G *et al* 1999 *Phys. Rev.* E **60** 5505
[24] Kob W *et al* 2000 *J. Phys.: Condens. Matter* **12** 6385
[25] Parisi G 1997 *Phys. Rev. Lett.* **79** 3660
[26] Sciortino F and Tartaglia P 2001 *Phys. Rev. Lett.* **86** 107
[27] Abraham F F 1980 *J. Chem. Phys.* **72** 359
[28] Oligschleger C and Schober H R 1999 *Phys. Rev.* B **59** 811
[29] Donati C *et al* 1998 *Phys. Rev. Lett.* **80** 2338
Donati C *et al* 1999 *Phys. Rev.* E **60** 3107
[30] Jund P, Rarivomanantsoa M and Jullien R 2000 *J. Phys.: Condens. Matter* **12** 8777
[31] Schirmacher W, Diezemann G and Ganter C 2000 *Physica* B **284–8** 1147
[32] Grigera T S *et al* 2001 *Phys. Rev. Lett.* **87** 085502